Table II. Important Bond Lengths/Å and Bond Angles/deg in $Zn_2Mo_3O_8$ and $Zn_2MoW_2O_8$

	$Zn_2Mo_3O_8$	$Zn_2MoW_2O_8$
(a) Coordination around Mo and Mo/W		
M-O(1)	2.00 (3)	2.022 (4)
M-O(2)	2.13 (3)	2.135 (3)
M-O(3) × 3	2.06 (1)	2.085 (2)
M-O(4) × 3	1.93 (2)	1.954 (2)
mean M-O	2.01	2.034
M-M (within cluster)	2.532 (2)	2.523 (3)
M-O(1)-M	78.2 (8)	77.2 (2)
M-O(4)-M	81.8 (5)	80.4 (1)
(b) Coordination around Zn		
Zn(1)-O(2)	1.99 (3)	2.015 (8)
Zn(1)-O(3) × 3	1.98 (1)	1.965 (3)
Zn(2)-O(3) × 3	2.12 (1)	2.176 (4)
Zn(2)-O(4) × 3	2.07 (2)	2.024 (4)

perature factors for Zn, W/Mo, and O were refined: $R_p = 9.15\%$, $R_{wp} = 10.33\%$, and $\chi^2 = 1.06$. In Table II, some important bond lengths in the $Zn_2MoW_2O_8$ structure are compared with the corresponding values in $Zn_2Mo_3O_8$. For this comparison, the fractional coordinates given in ref 6 were used, together with the more accurate lattice parameters obtained in the present work.

The most striking feature of our refinement is that the metal-metal single bond in the mixed triangular cluster is almost identical with, and probably slightly shorter than, the Mo-Mo distance in $Zn_2Mo_3O_8$. Extrapolating our results to the pure tungsten end-member, we would predict a W-W bond length of 2.518 Å. This trend is in agreement with the metal-metal distances in the distorted MO_2 rutile structures, with Mo-Mo = 2.5106 (5) Å[10] and W-W = 2.475 Å,[11] and with thermochemical estimates which suggest that W-W bonds are stronger than their molybdenum analogues.[12] The single-bond M-M distances in the triangular alkoxide clusters, $M_3O(OR)_{10}$ with R = *i*-Pr, which yield Mo-Mo = 2.534 (5) Å[13] and W-W = 2.540 (6) Å,[14] are also in good agreement with our results. On the other hand, it is interesting to recall that Mo-Mo bonds become significantly shorter than their W-W counterparts in complexes containing triple or quadruple M-M bonds.[15]

The similarity between the Mo-Mo and W-W bond lengths in the $Zn_2Mo_{3-x}W_xO_8$ system can be contrasted with the overall increase in cell volume, which reflects the fact that the W-O bonds are longer than Mo-O bonds. The marginal shortening of the M-M bond and the lengthening of M-O distances in the title compound result in the M-O(1)-M and M-O(4)-M angles becoming more acute (Table II); O(1) lies centrally above the cluster, and O(4) bridges the edges of the cluster.

We must now address the question as to why the tungsten oxide cluster compounds are unstable, in spite of the fact that W-W single bonds are apparently as short as, and therefore probably stronger than, Mo-Mo bonds. In this regard, it is instructive to examine the energetics of the disproportionation of MoO_2 and WO_2 according to the following equation:

$$3MO_2 \rightarrow 2MO_3 + M \qquad (2)$$

From thermochemical data for the corresponding dioxides and trioxides,[16,17] it can be shown that the heat of disproportionation of MoO_2 (+92.2 kJ mol^{-1}) is considerably higher than that of WO_2 (+27.5 kJ mol^{-1}), even though their heats of formation are almost identical. This result and the structural findings in the present work point to the conclusion that the instability of tungsten oxide cluster compounds stems not from the weakness of the W-W bonds but from the high sublimation energy of W metal and the relative ease with which tungsten is oxidized to the +VI oxidation state. These factors are consistent with decomposition pathways of the type shown in eq 1. If the behavior in the solid state is analogous to that in the coordination complexes, we would also expect that tungsten oxide clusters are even less likely to be found in phases that would require multiply bonded W-W interactions.

Acknowledgment. We thank the SERC for the provision of neutron diffraction facilities at ISIS, British Petroleum plc. for an EMRA grant, Dr. Bill Harrison for invaluable advice on the Rietveld software, and Prof. Malcolm Chisholm for some useful comments.

Supplementary Material Available: Table SI, listing atomic coordinates and isotropic temperature factors for Zn, Mo/W, and O (1 page). Ordering information is given on any current masthead page.

University of Oxford
Chemical Crystallography Laboratory
9 Parks Road, Oxford OX1 3PD, U.K.

Anthony K. Cheetham*
Simon J. Hibble
Helen R. Wakerley

Received August 30, 1988

---

(10) Brandt, B. G.; Skapski, A. C. *Acta Chem. Scand.* **1967**, *21*, 661-672.
(11) Palmer, D. J.; Dickens, P. G. *Acta Crystallogr., Sect. B: Struct. Crystallogr. Cryst. Chem.* **1979**, *35*, 2199-2201.
(12) Cotton, F. A. In *Reactivity of Metal-Metal Bonds*; Chisholm, M. H., Ed.; ACS Symposium Series 155; American Chemical Society: Washington, DC, 1981; pp 1-16.
(13) Chisholm, M. H.; Folting, K.; Huffman, J. C.; Kirkpatrick, C. C. *Inorg. Chem.* **1984**, *23*, 1021-1037.
(14) Chisholm, M. H.; Folting, K.; Huffman, J. C.; Kober, E. M. *Inorg. Chem.* **1985**, *24*, 241-245.
(15) Cotton, F. A.; Extine, M. W.; Felthouse, T. R.; Kolthammer, B. W. S.; Lay, D. G. *J. Am. Chem. Soc.* **1981**, *103*, 4040-4045.
(16) Mah, A. D. *J. Am. Chem. Soc.* **1959**, *81*, 1582-1583.
(17) Mah, A. D. *J. Phys. Chem.* **1957**, *61*, 1572-1573.

Synthesis and Structural Characterization of the First Gallacarborane Sandwich

We recently described a unique synthetic route leading to the *commo*-aluminacarborane sandwich, Tl[*commo*-3,3′-Al(3,1,2-$AlC_2B_9H_{11})_2$] (**1**).[1] As part of our continuing research effort with main-group metallacarboranes, we have attempted to expand this procedure to other group 13 metals. We now report the synthesis and single-crystal X-ray diffraction study of the first *commo*-gallacarborane sandwich, Tl[*commo*-3,3′-Ga(3,1,2-$GaC_2B_9H_{11})_2$] (**2**). Although minor differences exist between the preparative routes that lead to **1** and **2**, the results presented here support the mechanism proposed in the initial communication.

The addition of a toluene solution containing 2 molar equiv of gallium(III) chloride to a suspension of 1 molar equiv of $Tl_2[7,8\text{-}C_2B_9H_{11}]$ in toluene formed **2** in 100% yield based on carborane as determined by ^{11}B FTNMR. During the course of the reaction, the mixture became colorless and free of suspended solids. The product **2** was isolated in only 55% yield due to difficulties inherent in its separation from the other reaction products. Fractional crystallization of the reaction solution using heptane as the countersolvent first produced $TlGaCl_4$, followed by **2**.[2] The crystals of **2** obtained by this means proved to be suitable for a single-crystal X-ray diffraction study. The ^{11}B FTNMR, ^1H FTNMR, and IR spectra of **2** were characteristic of a compound that contains a single type of symmetric carborane cage. The formulation $Tl[Ga(C_2B_9H_{11})_2]$ was confirmed by elemental

---

(1) Bandman, M. A.; Knobler, C. B.; Hawthorne, M. F. *Inorg. Chem.* **1988**, *27*, 2399.
(2) $GaCl_3$ (325 mg, 1.85 mmol) was dissolved in approximately 100 mL of toluene in the glovebox. This solution was added to a suspension of $Tl_2(7,8\text{-}C_2B_9H_{11})$ (500 mg, 0.92 mmol) in toluene and the mixture stirred. After 1 h, the solution became homogeneous and colorless. The final product was isolated by fractional crystallization using heptane as the countersolvent. The composition of the material isolated was monitored by mass spectroscopy (the disappearance of the *m/e* peaks due to $TlGaCl_4$) and IR spectroscopy (the appearance of the B-H stretching vibration due to the carborane cage of **2** at 2522 cm^{-1}). When $TlGaCl_4$ was no longer observable the product was washed with heptane yielding 136 mg (55%) of colorless, crystalline **2**.

0020-1669/89/1328-1204$01.50/0

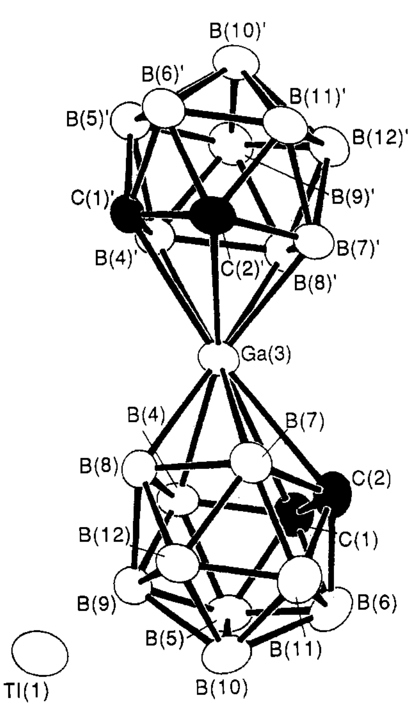

Figure 1. ORTEP representation of compound **2** with hydrogen atoms omitted for clarity, showing the numbering scheme. Interatomic distances in Å: Ga–C(1), 2.565 (7); Ga–C(2), 2.591 (8); Ga–B(4), 2.265 (8); Ga–B(7), 2.297 (8); Ga–B(8), 2.083 (8); Ga–C(1′), 2.481 (7); Ga–C(2′), 2.492 (7); Ga–B(4′), 2.253 (8); Ga–B(7′), 2.251 (8); Ga–B(8′), 2.095 (8).

analysis and mass spectroscopy giving mass envelopes that corresponded to $TlGaC_2B_9H_{11}^+$, $GaC_4B_{18}H_{22}^+$, and $GaC_2B_9H_{11}^+$ overlapped with Tl^+.[3] Hydrolysis of **2** proceeds rapidly, producing the [*nido*-7,8-$C_2B_9H_{11}]^-$ anion.

The structure of sandwich **2** was elucidated by X-ray diffraction[4] and is presented in Figure 1. This structural study highlights several differences between this gallacarborane and the analogous aluminacarborane sandwich. Interestingly, whereas compound **1** clearly contains an η^5-bound metal center, the gallium atom in compound **2** is noticeably slipped toward the three boron atoms in each of the bonding faces in such a manner as to suggest η^3-bonding. These two carborane ligands would then donate 4 electrons each, resulting in a total of 8 electrons in the valence shell of the formal gallium(III) center. As an illustration of the magnitude of the observed lateral distortion, the slipping parameter Δ, as defined by Mingos,[5] was calculated with the following results:[6] prime cage, 0.49 Å; nonprime cage, 0.60 Å; cage A of **1**, 0.29 Å; cage B of **1**, 0.24 Å. For purposes of comparison, only one other gallacarborane structure, that for *closo*-3-CH_3-3,1,2-$GaC_2B_4H_6$ (**3**),[7] has been structurally characterized by crystallographic methods (the 12-vertex gallacarborane *closo*-3-CH_3CH_2-3,1,2-$GaC_2B_9H_{11}$[8] was synthesized and characterized by spectroscopic methods). The species **3** displayed a similar, but less pronounced slippage. Since compound **3** contains only one pentagonal ring, Δ could not be calculated. However, the displacement of the gallium center from the normal to the bonding plane at the centroid of **3** was found to be 0.24 Å. The corresponding displacements for **2** were 0.43 Å for the prime cage and 0.53 Å for the nonprime cage. Previous authors[7,9] suggest that these structural characteristics were due to back-bonding from filled d orbitals into nonbonding MO's originating in the carborane ligand. More recently, however, Canadell, Eisenstein, and Rubio[10] have performed theoretical calculations on **3** suggestive of an alternative interpretation, which in turn has received further support from Hosmane and Maguire.[11] The latter theory depends only upon optimized gallium s- and p-orbital interactions with carborane molecular orbitals and requires no d-orbital participation to explain the slippage of the Ga atom from the normal to the centroid of the plane, as well as the observed tilt of the CH_3–Ga axis from the normal to the plane in **3**. A similar argument could explain the observed slippage in **2**.

Another unusual aspect of the structure of **2** was the eclipsed conformation of the two carborane cages. While the majority of carborane sandwich compounds adopt a staggered transoid conformation, with carbons on opposing cages as far from each other as possible, a slight rotation from this ideal conformation in **2** places atoms on opposite cages in a congruent relationship. Bridged bis(dicarbollide) cobaltacarboranes also exhibit this anomaly, most likely due to the hindered rotation caused by the bridge.[12] In the present case, we believe nonbonded interactions of carborane hydrogen atoms with a thallium cation produce the observed distortion. Each thallium cation in the unit cell was surrounded by five gallacarborane ions, contributing a total of six cage hydrogen atoms that approach to within 3.2 Å. As a result of the rotation of the ligands, the sandwich must be distorted to achieve maximum overlap of gallium atomic orbitals with cage molecular orbitals. The angle between the normals to the planar open faces of the carborane ligands was 174.5°.

Although we were unable to isolate any of the reaction byproducts from the synthesis of the aluminum sandwich, we were able to secure such materials during the synthesis of the gallium analogue. The only other species formed in this reaction was thallium tetrachlorogallate, which was isolated as the crystalline phase initially formed upon layering the reaction solution with heptane. X-ray crystallography[13] and mass spectroscopy[14] confirmed the identity of these crystals as $TlGaCl_4$. Consequently, the reaction must proceed in accord with

---

(3) Spectroscopic and analytical data for **2**. IR spectrum (Nujol): 2522 (s), 1094 (w), 1023 (w), 980 (w) cm^{-1}. ^1H FTNMR (200.133 MHz) (C_7D_8, referenced to residual solvent protons = 7.15 ppm): 2.72 ppm (s, carborane CH). $^{11}B\{^1H\}$ FTNMR (160.463 MHz) (C_7H_8; referenced to external $BF_3 \cdot OEt_2$ in C_6D_6): −13.11, −15.40, −17.61, −25.01, −31.16 ppm. Mass spectrum (reported as the strongest *m/e* peak in each mass envelope consisting of various isotopic combinations of the given formula): $TlGaC_2B_9H_{11}^+$, 407; $GaC_4B_{18}H_{22}^+$, 333; $^{205}Tl^+$, 205; $GaC_2B_9H_{11}^+$ and $^{203}Tl^+$, 203. Anal. Calcd for $TlGaC_4B_{18}H_{22}$: C, 8.92; H, 4.08; B, 36.12; Tl, 37.94; Ga, 12.94. Found: C, 8.06; H, 3.71; B, 35.20; Tl, 38.18; Ga, 13.20.

(4) Colorless parallelepiped X-ray quality crystals were obtained from a toluene/mesitylene solution layered with heptane. A crystal was placed in a 0.3-mm capillary tube in a drybox under Ar and sealed. Data collection was carried out at 25 °C, by using a locally designed automated diffractometer (Mo Kα radiation). The space group was $P\bar{1}$ with $a = 6.9564$ (6) Å, $b = 11.0466$ (9) Å, $c = 12.0287$ (10) Å, $\alpha = 102.088$ (2)°, $\beta = 95.484$ (2)°, $\gamma = 94.687$ (3)°, $V = 894$ Å^3, and $Z = 2$. A total of 2733 reflections with $I > 3\sigma(I)$ were used for structure solution and refinement with the heavy-atom method and the UCLA crystallographic package. The unit cell contains two $Tl^+[Ga(C_2B_9H_{11})_2]^-$ molecules. The last cycle of least-squares refinement gave residuals of $R = 0.041$, $R_w = 0.064$, and GOF = 1.57.

(5) Mingos, D. M.; Forsyth, M. I.; Welch, A. *J. Chem. Soc., Chem. Commun.* **1977**, 605.

(6) The terms "prime cage" and "nonprime cage" refer to the carborane ligands of **2** as designated in the figure by primed and nonprimed numbers, respectively. "Cage A" and "cage B" refer to two crystallographically different molecules contained in the unit cell of **1**. A third molecule of **1** in the unit cell was disordered and thus was not used for these comparisons.

(7) Grimes, R. N.; Rademaker, W. J.; Denniston, M. L.; Bryan, R. F.; Greene, P. T. *J. Am. Chem. Soc.* **1972**, *94*, 1865.

(8) Young, D. A. T.; Wiersema, R. J.; Hawthorne, M. F. *J. Am. Chem. Soc.* **1971**, *93*, 5687.

(9) Warren, L. F., Jr.; Hawthorne, M. F. *J. Am. Chem. Soc.* **1968**, *90*, 4823.

(10) Canadell, E.; Eisenstein, O.; Rubio, J. *Organometallics* **1984**, *3*, 759.

(11) Hosmane, N. S.; Maguire, J. A. In *Molecular Structure and Energetics*; Liebman, J. F.; Greenberg, A., Williams, R. E., Eds.; VCH: New York, 1988; Vol. 5, pp 197–328.

(12) (a) Shelly, K.; Knobler, C. B.; Hawthorne, M. F. *New J. Chem.* **1988**, *12*, 317. (b) Subrtova, V.; Petricek, V.; Linek, A.; Jecny, J. *Z. Kristallogr., Kristallgeom., Kristallphys., Kristallchem.* **1976**, *144*, 139. (c) Petrina, A.; Petricek, V.; Maly, K.; Subrtova, V.; Linek, A.; Hummel, L. *Z. Kristallogr., Kristallgeom., Kristallphys., Kristallchem.* **1981**, *154*, 217.

(13) An X-ray diffraction analysis of $TlGaCl_4$ was published previously: Meyer, G.; Schwan, E. *Z. Naturforsch.* **1980**, *35B*, 117.

(14) Mass envelope observed for $TlGaCl_3^+$.

$$2Tl_2C_2B_9H_{11} + 4GaCl_3 \rightarrow Tl[Ga(C_2B_9H_{11})_2] + 3TlGaCl_4$$

This equation is analogous to that proposed for the synthesis of the aluminum sandwich from the reaction of an alkylaluminum chloride with $Tl_2[7,8-C_2B_9H_{11}]$ which produced thallium salts of alkylchloroaluminates. Attempts to synthesize compound 2 by using alkylgallium reagents were unsuccessful. Work continues on the group 13 metallacarboranes including indium and thallium and will be reported elsewhere.

Acknowledgment. The support of this work by the National Science Foundation (Grant CHE-88-06179) is gratefully acknowledged.

Supplementary Material Available: Tables of positional and thermal parameters and interatomic distances and angles (7 pages). Ordering information is given on any current masthead page.

Department of Chemistry
and Biochemistry
University of California
Los Angeles, California 90024-1569

Marc A. Bandman
Carolyn B. Knobler
M. Frederick Hawthorne*

Received December 9, 1988

A Ligand-Imposed Cradle Geometry for a Dicobalt Tetracarbonyl Tetratertiary Phosphine Complex

Most transition-metal dimers bridged by two bis(phosphino)methane-type linkages adopt a geometry in which the two $R_2PCH_2PR_2$ ligands are oriented trans to one another and are commonly referred to as A-frames.[1,2] A few bimetallic complexes have the two $R_2PCH_2PR_2$ ligands in a cisoidal bridging arrangement,[3] which have been referred to as W-frame[4] or cradle[5] geometries. The A-frame geometry has been compared to a flat metal catalyst surface, while the cradle geometry correlates to the more reactive edge or kink of a metal.[6] Unfortunately, aside from working with metal atoms that have tetrahedral coordination geometries which require a cisoidal orientation of two bis(phosphino)methane ligands, methods for the rational preparation of this unusual ligand arrangement are lacking.

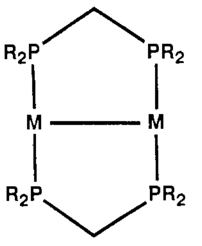

trans,trans-$M_2(R_2PCH_2PR_2)_2$
"A-Frame"

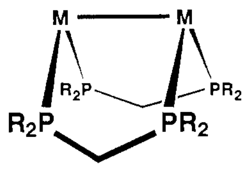

cis,cis-$M_2(R_2CH_2PR_2)_2$
"Cradle"

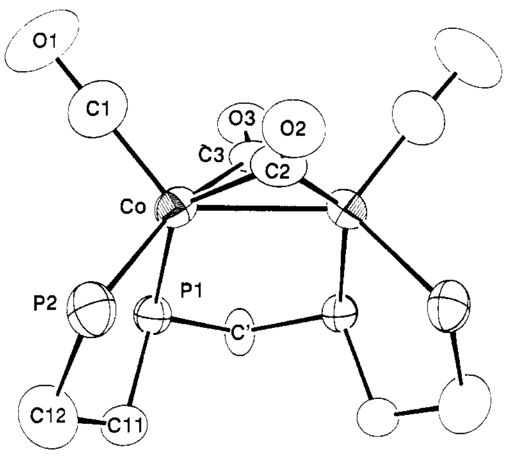

Figure 1. ORTEP plot of *meso*-$Co_2(\mu\text{-}CO)_2(CO)_2$(eLTTP) (1), with the phenyl and terminal ethyl groups removed for clarity. The molecule lies on a crystallographic mirror plane that passes through the bridging carbonyl ligands and the central methylene bridge of eLTTP. Ellipsoids are shown at the 33% probability level. Important bond distances (Å) and angles (deg): Co–Co′ = 2.513 (4), Co–P1 = 2.212 (4), Co–P2 = 2.236 (4), Co–C1 = 1.73 (2), Co–C2 = 1.93 (2), Co–C3 = 1.92 (2); P1–Co–P2 = 85.2 (2), P1–Co–C1 = 118.0 (6), P1–Co–C2 = 138.7 (5), P1–Co–C3 = 87.1 (5), P2–Co–C1 = 97.6 (6), P2–Co–C2 = 94.7 (6), P2–Co–C3 = 167.5 (5), C1–Co–C2 = 102.9 (8), C1–Co–C3 = 94.7 (7), C2–Co–C3 = 84.8 (7), P1–C′–P1′ = 111.5 (8).

Our synthesis of the powerful binucleating linear tetrakis(phosphine) ligand $(Et_2PCH_2CH_2)(Ph)PCH_2P(Ph)(CH_2CH_2PEt_2)$, eLTTP, which exists as racemic and meso diastereomers, has produced a structurally characterized open-mode Rh(I) bimetallic complex with the racemic ligand.[7] Molecular models of *meso*-eLTTP suggest that for bimetallic complexes with M–M bonds this ligand must adopt a cradle-like arrangement of the four phosphine ligands around the metal centers. Herein, we report the synthesis and structural characterization of the Co(0) dimer *meso*-$Co_2(\mu\text{-}CO)_2(CO)_2$(eLTTP), which has the predicted cradle geometry.

The reaction of $Co_2(\mu\text{-}CO)_2(CO)_2(\text{norbornadiene})_2$[8] with eLTTP in cyclohexane produces a dark orange-brown mixture of the racemic and meso diastereomeric dimer complexes that analyzes as $Co_2(CO)_4$(eLTTP).[9] Slow evaporation of a THF solution crystallizes a diamagnetic orange material that has terminal and bridging ν_{CO} bands at 1925 and 1720 cm^{-1}. These bands are similar to those seen in the dppe-substituted dimer $Co_2(\mu\text{-}CO)_2(CO)_2(dppe)_2$ (dppe = $Ph_2PCH_2CH_2PPh_2$).[10] The ^{31}P NMR spectrum also suggests a symmetrical Co–Co-bonded eLTTP-substituted species with cobalt quadrupole-broadened resonances at 64.5 and 84.4 ppm.

---

(1) Cf.: (a) Olmstead, M. M.; Hope, H.; Brenner, L. S.; Balch A. L. *J. Am. Chem. Soc.* **1977**, *99*, 5502. (b) Kubiak, C. P.; Eisenberg, R. *J. Am. Chem. Soc.* **1977**, *99*, 6129. (c) Cowie, M.; Mague, J. T.; Sanger, A. R. *J. Am. Chem. Soc.* **1978**, *100*, 3628. (d) Brown, M. P.; Fisher, J. R.; Puddephatt, R. J.; Seddon, K. R. *Inorg. chem.* **1979**, *18*, 2808. (e) Kubiak, C. P.; Eisenberg, R. *J. Am. Chem. Soc.* **1980**, *102*, 3637.

(2) For the most recent review article on A-frame complexes see: Kubiak, C. P. *Polyhedron*, submitted for publication.

(3) (a) DeLaet, D. L.; del Rosario, R.; Fanwick, P. E.; Kubiak, C. P. *J. Am. Chem. Soc.* **1987**, *109*, 754. (b) Berry, D. H.; Eisenberg, R. *Organometallics* **1987**, *6*, 1796. (c) Cotton, F. A.; Dunbar, K. R.; Verbruggen, M. G. *J. Am. Chem. Soc.* **1987**, *109*, 5498. (d) Wu, J.; Fanwick, P. E.; Kubiak, C. P. *J. Am. Chem. Soc.* **1988**, *110*, 1319.

(4) Karsch, H. H.; Milewski-Mahrla, B.; Besenhard, J. O.; Hofman, P.; Stauffert, P.; Albright, T. A. *Inorg. Chem.* **1986**, *25*, 3811.

(5) DeLaet, D. L.; Fanwick, P. E.; Kubiak, C. P. *Organometallics* **1986**, *5*, 1807.

(6) Osborn, J. A.; Stanley, G. G.; Bird, P. H. *J. Am. Chem. Soc.* **1988**, *110*, 2117.

(7) Laneman, S. A.; Fronczek, F. R.; Stanley, G. G. *J. Am. Chem. Soc.* **1988**, *110*, 5585.

(8) Winkhaus, G.; Wilkinson, G. *J. Chem. Soc.* **1961**, 602.

(9) All manipulations were carried out under inert-atmosphere conditions with appropriately dried and degassed solvents. A 0.232-g (0.5-mmol) sample of eLTTP[7] in 20 mL of cyclohexane is added to a suspension of 0.207 g (0.5 mmol) of $Co_2(\mu\text{-}CO)_2(CO)_2(\text{norbornadiene})$[8] in 30 mL of cyclohexane and the mixture refluxed for 15 h. During this time the solution changes from an orange slurry to a dark purplish brown solution with a fair amount of dark precipitate. The dark brown precipitate, which is a mixture of *rac*- and *meso*-$Co_2(CO)_4$(eLTTP) diastereomers, is collected and washed with cyclohexane to give an overall yield of ca. 60–70% (ca. 30–35% yield of the meso diastereomer). The solid is very soluble in THF, benzene, and CH_2Cl_2; slightly soluble in acetone, diethyl ether, toluene, acetonitrile, and MeOH; and insoluble in hexane and H_2O. Orange crystals that initially form from the slow evaporation of a THF solution are *meso*-$Co_2(\mu\text{-}CO)_2(CO)_2$(eLTTP). IR (KBr, ν_{CO}): 1925 (s) and 1720 (m) cm^{-1}. ^{31}P NMR (toluene-d_8, ppm, H_3PO_4 reference): 64.46 and 84.35 (P–P couplings are obscured by quadrupolar relaxation from the cobalt atoms). Satisfactory analytical data (C, H) were obtained on recrystallized samples of 1 (Oneida Research Services, Whitesboro, NY).

(10) Behrens, V. H.; Aquila, W. *Z. Anorg. Allg. Chem.* **1967**, *356*, 8.